

# Convolutional Neural Network-based Media Noise Prediction and Equalization for TDMR Turbo-detection with Write/Read TMR

Amirhossein Sayyafan<sup>1</sup>, Ahmed Aboutaleb<sup>1</sup>, Benjamin Belzer<sup>1</sup>, Krishnamoorthy Sivakumar<sup>1</sup>, Simon Greaves<sup>2</sup>

<sup>1</sup>Washington State University, Pullman, WA, USA, (a.sayyafan, ahmed.aboutaleb, belzer, siva)@wsu.edu

<sup>2</sup>RIEC, Tohoku University, Sendai 980-8577, Japan, simon@riec.tohoku.ac.jp

This paper presents a turbo-detection system consisting of a convolutional neural network (CNN) based equalizer, a Bahl–Cocke–Jelinek–Raviv (BCJR) trellis detector, a CNN-based media noise predictor (MNP), and a low-density parity-check (LDPC) channel decoder for two-dimensional magnetic recording (TDMR). The BCJR detector, CNN MNP, and LDPC decoder iteratively exchange soft information to maximize the areal density (AD) subject to a bit error rate (BER) constraint. Simulation results employing a realistic grain switching probabilistic (GSP) media model show that the proposed system is quite robust to track-misregistration (TMR). Compared to a 1-D pattern-dependent noise prediction (PDNP) baseline with soft intertrack interference (ITI) subtraction, the system achieves 0.34% AD gain with read-TMR alone and 0.69% with write- and read-TMR together.

**Index Terms**—Turbo-detection, two-dimensional magnetic recording, convolutional neural network, CNN media noise prediction, CNN Equalizer.

## I. INTRODUCTION

THE DETECTION of two-dimensional magnetic recording (TDMR) is considered in the presence of disturbances to the positions of the writer and reader. The disturbances, referred to as track-misregistration (TMR), are modeled as relatively slowly-varying random processes. These are taken as independent track-to-track during writing and independent during reading but with the three readers ganged together. Due to these disturbances, the detector must deal with time-varying intertrack interference (ITI). In the present work, since TDMR signals are viewed as 2-D images, a convolutional neural network (CNN) based media noise prediction and equalizer are utilized in a turbo-detection system to mitigate the effect of TMR. Performance is compared with pattern-dependent noise prediction (PDNP), commonly employed in hard disc drives (HDD) [1].

## II. SYSTEM MODEL

Shingled magnetic recording (SMR) waveforms are generated using the grain switching probabilistic (GSP) model [2], [3]. Fig. 1 shows the cross track geometry. Signals are available for tracks  $\mathbf{a}_1$ ,  $\mathbf{a}_2$ , and  $\mathbf{a}_3$  at read offsets from  $-3$  nm to  $+3$  nm in  $1$  nm steps. The positions of the four center written tracks can also be varied. The nominal track pitch (TP) and bit length (BL) are  $24$  and  $10$  nm respectively (approximately  $2.7$  terabits per square inch ( $\text{Tb/in}^2$ ) uncoded areal density (AD)).

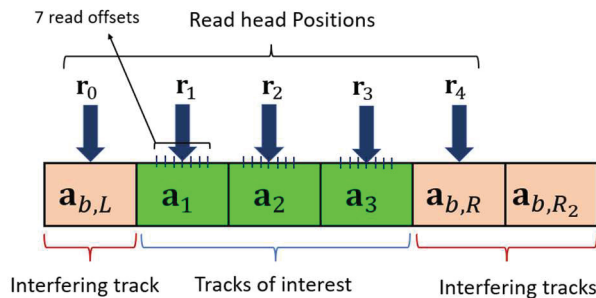


Fig. 1. Cross-track view of the GSP data geometry. Signals from the five readers are available simultaneously.

## III. READ- AND WRITE-TMR MODEL

For the read-TMR, we consider only write-to-read misregistration. The written tracks are assumed to be placed perfectly (i.e., no write-to-write TMR); all three read-heads move simultaneously. We use multi-track GSP based simulated read-head data at various reader offsets from the track center, with resolution of  $1$  nm.

We synthesize position errors by driving a first order LPF,  $H(z) = \frac{1-\alpha}{1-\alpha z^{-1}}$  with an i.i.d. Gaussian random process. The down-track coherence length of the TMR is controlled by the value of  $\alpha$  which is set such that the impulse response falls to  $0.5$  after about  $66000$  bits corresponding to about two  $4$  KByte sectors. Fig. 2(a) is an example of the position error disturbance, and Fig. 2(b) shows the read-head model in which the readers are moving as a group (ganged together).

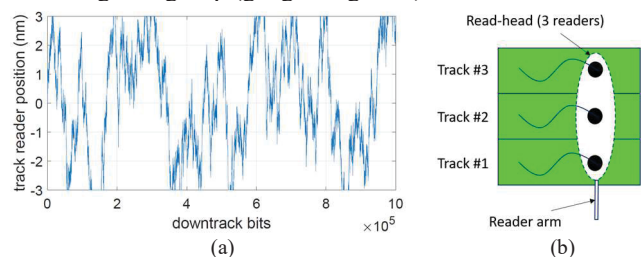


Fig. 2. (a) Example of position error used in the simulations. The actual disturbance is quantized to the  $7$  integer nanometer values from  $-3$  nm to  $+3$  nm. (b) read-head model.

For the write-TMR, the positions of tracks  $\mathbf{a}_1$ ,  $\mathbf{a}_2$ ,  $\mathbf{a}_3$ , and  $\mathbf{a}_{b,R}$  are varied independently while  $\mathbf{a}_{b,L}$  and  $\mathbf{a}_{b,R_2}$  are fixed. Since the individual disturbances are truncated at  $\pm 3$  nm, the extreme variation in TP is  $\pm 6$  nm. The write-TMR GSP model first creates the sets of  $6$  adjacent  $4$  KByte blocks in all of the possible  $7^4 = 2401$  written track positions. Readback waveforms are then created for each with  $7$  possible reader positions. The three readers are ganged together nominally covering tracks  $\mathbf{a}_1$ ,  $\mathbf{a}_2$ , and  $\mathbf{a}_3$  for a total of  $16807$  possible sets of waveforms to sample from. Then the addition, independently, of the additive white Gaussian noise adds a further degree of randomization. In Fig. 3, track centers  $1$ ,  $2$ ,  $3$ , and  $4$  are shifted by  $+3$ ,  $-3$ ,  $-3$ ,  $+3$  nm respectively. By providing all possible

combinations of write-head position we can construct a correlated write-head position TMR random process.

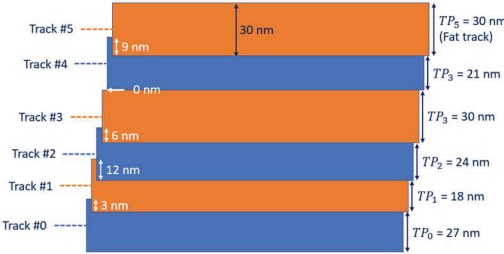


Fig. 3. Position error due to the write-TMR.

#### IV. BCJR-LDPC-CNN TURBO-DETECTOR

Fig. 4 illustrates the BCJR-LDPC-CNN turbo-detection system. The intersymbol interference (ISI) detection and media noise prediction functions are separated into two detectors using turbo equalization. The read samples  $\mathbf{r}$  are passed to a 2-D MMSE partial response (PR) equalizer with target  $\mathbf{h}$ . The 2-D BCJR trellis detector performs ISI/ITI equalization on input  $\mathbf{y}$ , generates log-likelihood ratios (LLRs)  $\mathbf{LLR}_{b_0}$  and passes them to the CNN. The CNN estimates the media noise  $\hat{\mathbf{n}}_m$  and feeds it back to the 2-D BCJR to obtain a lower bit error rate (BER). Next, the 2-D BCJR passes LLRs  $\mathbf{LLR}_b$  to a low-density parity check (LDPC) decoder. The decoder generates the final LLRs  $\mathbf{LLR}_l$  after each turbo-iteration [3], [4].

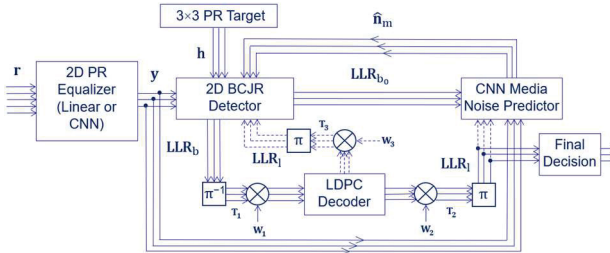


Fig. 4. Block diagram of the turbo-detection system.

##### A. Linear and CNN Equalizer Designs

The linear PR equalizers minimize the mean-squared error (MSE) between ideal PR signals and the equalizer output. The CNN equalizer takes five reading sequences  $\mathbf{r}_0, \dots, \mathbf{r}_4$  to generate the equalized waveforms  $\mathbf{y} = [\mathbf{y}_1, \mathbf{y}_2, \mathbf{y}_3]$  for the three central tracks. Readings within a  $5 \times 17$  sliding window are used for equalizing the reading samples. The equalizer uses a  $3 \times 3$  PR target. For the fixed CNN equalizer, the constrained MSE solver optimizes the PR target mask. For a fixed PR target, using stochastic gradient descent, the CNN equalizer weights are adjusted to minimize the average MSE between its output and the ideal PR waveforms. This iterative method jointly optimizes the CNN equalizer weights and the PR target [3].

##### V. 1-D PDNP WITH LLR EXCHANGE

In this case, there are three parallel 1-D BCJR/PDNP detectors operating on tracks  $\mathbf{a}_1, \mathbf{a}_2$ , and  $\mathbf{a}_3$ . LLRs are passed from the two outer tracks to the inner track. The central 1-D BCJR/PDNP uses weights  $\alpha_1$  and  $\alpha_3$  for mapping the expected value of coded bits ( $\mathbf{u}_1, \mathbf{u}_3$ ) from the other tracks' 1-D BCJR/PDNP LLRs:

$$\min_{\alpha_1, \alpha_3} \|\mathbf{y}_2 - (\mathbf{h}_2 * \mathbf{u}_2 + \alpha_1 * \mathbf{s}_1 + \alpha_3 * \mathbf{s}_3)\|^2,$$

$s_i = (\exp(\mathbf{LLR}_i) - 1)/(\exp(\mathbf{LLR}_i) + 1)$ ,  $i = 1, 3$ , (1) where  $\mathbf{h}_2$  is the  $1 \times 3$  PR target and  $\mathbf{u}_2$  are the coded bits on the central track. The  $\mathbf{s}_i$  is the expected value of each bit in the outer tracks, and  $*$  indicates convolution. In this system, the BER and AD are assessed on  $\mathbf{a}_2$ . By introducing this exchange of suitably weighted LLRs, the central track's MSE decreases by 8.85% in presence of write- and read-TMR.

#### VI. RESULTS AND DISCUSSION

Table I presents the simulation results for the read-TMR alone (written tracks fixed at nominal, each track with 7 possible read offsets from  $-3$  nm to  $+3$  nm). Rows 1, 3 serve as comparison baseline (cb). In most cases, the CNN-based system gives some density gain over the PDNP systems. The CNN-based system gives 0.34% density gain over PDNP with LLR exchange and is more robust with read-TMR alone.

TABLE I  
READ-TMR SIMULATION RESULTS, TP = 24 NM

Detector	AD (Tb/in <sup>2</sup> )	Code Rate	AD Reduction (%)
1-D PDNP, LLR Exch. (cb. 1)	2.3922	0.8899	0
1-D PDNP, LLR Exch., R TMR	2.2937	0.8533	4.11 (vs cb. 1)
CNN NP (cb. 2)	2.3880	0.8883	0
CNN NP, R TMR	2.3016	0.8562	3.61 (vs cb. 2)

For the write-TMR dataset selection, we generate four independent waveforms with maximum TMR of  $\pm 3$  nm. The training and validation datasets comprise 400 and 100 four KByte blocks respectively; 200 additional independently generated blocks are used as test data. Table II shows the simulation results for the write-TMR alone and for write- and read-TMR together. The LLR exchange improves density and robustness to TMR for the PDNP system. The system with the CNN Equalizer gains 0.69% density over PDNP with LLR exchange in the presence of write- and read-TMR. The CNN system with the CNN Equalizer improves density and robustness compared to PDNP.

TABLE II  
WRITE- AND READ-TMR SIMULATION RESULTS, TP = 24 NM

Detector	AD (Tb/in <sup>2</sup> )	Code Rate	AD Reduction (%)
1-D PDNP, LLR Exch., W TMR	2.2440	0.8347	6.20 (vs cb. 1)
1-D PDNP, LLR Exch., W-R TMR	2.1795	0.8108	8.89 (vs cb. 1)
CNN NP, W TMR	2.2695	0.8443	4.95 (vs cb. 2)
CNN NP, CNN Eq., W TMR	2.2793	0.8479	4.55 (vs cb. 2)
CNN NP, CNN Eq., W-R TMR	2.1947	0.8164	8.09 (vs cb. 2)

This work is funded by NSF grant CCF-1817083 and by the Advanced Storage Research Consortium (ASRC). The authors thank Dr. Roger Wood for his advice and suggestions.

#### REFERENCES

- [1] J. Moon and J. Park, "Pattern-dependent noise prediction in signal dependent noise," *IEEE Jour. Sel. Areas Commun.*, vol. 19, no. 4, pp. 730–743, Apr 2001.
- [2] S. Greaves, K. S. Chan, and Y. Kanai, "Areal Density Capability of Dual-Structure Media for Microwave-Assisted Magnetic Recording," *IEEE Trans. Mag.*, vol. 55, no. 12, Dec. 2019, 6701509.
- [3] A. Sayyafan, et al., "Deep Neural Network Media Noise Predictor Turbo-detection System for 1-D and 2-D Dimensional High-Density Magnetic Recording," *IEEE Trans. Mag.*, vol. 57, no. 3, March 2021, 3101113.
- [4] A. Sayyafan, et al., "Turbo-Detection for Multilayer Magnetic Recording Using Deep Neural Network-Based Equalizer and Media Noise Predictor," *IEEE Trans. Mag.*, vol. 58, no. 4, April 2022, 3200611.